ELSEVIER

Journal of Nuclear Materials 282 (2000) 137–145

journal of nuclear materials

www.elsevier.nl/locate/jnucmat

Preparation of uranium by electrolysis in chloride melt

K. Serrano [a], P. Taxil [a,*], O. Dugne [b], S. Bouvet [c], E. Puech [d]

[a] *Laboratoire de Génie Chimique, Universite Paul Sabatier, U.M.R. 5503, 118 route de Narbonne, 31062 Toulouse cedex 04, France*
[b] *Commissariat à l'Energie Atomique, Centre de la vallée du Rhône, B.P. 111, Pierrelatte cedex 26702, France*
[c] *Pechiney Centre de Recherches de Voreppe, Parc Economique Centr'Alp B.P. 27, 38340 Voreppe, France*
[d] *Laboratoire des Interactions Moléculaires et Réactivité Chimiques et Photochimiques, U.M.R. 5623, 118 route de Narbonne, 31062 Toulouse cedex 04, France*

Received 13 December 1999; accepted 15 September 2000

Abstract

The uranium deposits were prepared by electrolysis in a fused chloride melt. Whatever the electrolysis conditions, the deposit morphology was dendritic. The influence of the parameters current density, melt temperature and electrolyte concentration on the morphology was investigated using an optimal design. Our results show that increasing the temperature makes the coatings more compact. The dendritic morphology is attributed to transport phenomena (diffusion, convection, migration) promoted by the cation discharge at the substrate-coating interface. © 2000 Elsevier Science B.V. All rights reserved.

1. Introduction

Electrochemical deposition in molten salts now is possible for the preparation of uranium [1–5]. The present work is focused on this topic.

We will first report previous works on the electrodeposition of uranium in chloride media.

In 1930, Driggs and Lilliendhal [1] reported the first preparation of metallic uranium by the electrolysis of a molten salt solution (NaCl–$CaCl_2$). A 'tree-like' deposit of this metal was obtained. They showed by chemical analysis that the deposit was extremely pure.

Kolodney [2], within the framework of the Manhattan Project, confirmed that uranium could be deposited by electrolysis of chloride melts such as ($BaCl_2$–KCl–NaCl–UCl_3). The best results concerning the current efficiency of the electrolysis and the purity of the deposited metal were obtained with a uranium concentration of 25–35 mass%. Kolodney observed that the deposit was dendritic, bright and malleable.

Marzano and Noland (Argonne National Laboratory) [3] using electrolytes KCl–$BaCl_2$–UCl_3 at 600–625°C and LiCl–KCl at 390–625°C and various substrates such as stainless steel and nickel alloys obtained dendritic deposits with high purity (99.9%) and current efficiencies about 50–60%. Examination of dendritic crystals revealed that they grow preferentially in the [310] direction. These authors pointed out that they could not obtain smooth coatings with thicknesses exceeding a few tenths of a micrometer, even though many experimental conditions were tested, such as rotating the cathode to lower the thickness of the diffusion layer, adding impurities to the melt, substituting fluorides for chlorides as electrolyte, using current reversal.

The Argonne National Laboratory went on with these studies in the 1980s. The objective was to obtain uniform deposits without dendrites: Marshall et al. [4] observed that the morphology of the coating is influenced neither by the cathode materials (tantalum, nickel, aluminium, iron, copper and stainless steel) nor by the concentration of UCl_3 in the 12–20 mass% range. However, they obtained more compact deposits when they used potentiostatic pulses for electrodeposition.

Finally, a detailed investigation of the coating morphology in LiCl–KCl was carried out by Totemeier and Mariani [5] using scanning electron microscopy in order

---

[*] Corresponding author. Tel.: +33-5 61 55 82 07; fax: +33-5 61 55 61 39.
E-mail address: taxil@ramses.ups-tlse.fr (P. Taxil).

0022-3115/00/$ - see front matter
PII: S0022-3115(00)00423-2

to determine the effect of zirconium in the feed material on the cathodic product.

The literature cited above does not report a significant influence of experimental conditions of electrolysis on the dendritic morphology of uranium coatings; even though, it has been shown in other systems that electrokinetic parameters such as concentration of the electrolyte, applied potential (or current) and melt temperature may influence the dendrite formation processes and growth rates [6–8].

This paper reports an investigation of the electrodeposition of uranium in a higher temperature range 670–710°C, using the NaCl–KCl–UCl_3 mixture as electrolyte, and includes certain results obtained in a previous electrochemical analysis of this system [9,10].

The influence of the electrokinetic parameters on the morphology of the uranium deposit was first studied using an optimal design to rationalize the experimental runs. Secondly, considering that the cathodic material could play an important role on the adherence of a coating, we observed the underlayer of the uranium deposit on various substrates. Finally, coating growth was studied to identify the physical phenomena acting on the development of the dendrites and their geometric shape. This work relied on SEM micrographic analysis like the work of Mariani and Totemeier [5].

2. Experimental procedures

2.1. The cell, the electrodes and the electrolyte

A vitreous carbon crucible containing the electrolyte was placed in a cylindrical refractory steel chamber where the inside wall was protected by a graphite liner. The cell was closed with a water-cooled stainless steel lid.

The experiments were performed in an inert U-grade argon atmosphere previously dehydrated and deoxygenated using a purification cartridge (Air liquide).

Taking into account the temperature range of the experimental work (670–710°C), the solvent used was an equimolar NaCl–KCl mixture, which melts at 658°C; trivalent uranium was obtained by dissolving UCl_4 in the melt and placing uranium metal in the form of small granules in the crucible. As observed in a previous work [9], the reduction of U^{IV} into U^{III} by uranium metal is complete:

$$3UCl_4 + U \rightarrow 4UCl_3 \tag{1}$$

The melt was initially dehydrated by heating the mixture of salts up to its melting point (658°C) under vacuum (4×10^{-2} mbar). The solute was then introduced into the melt through an air-lock under argon.

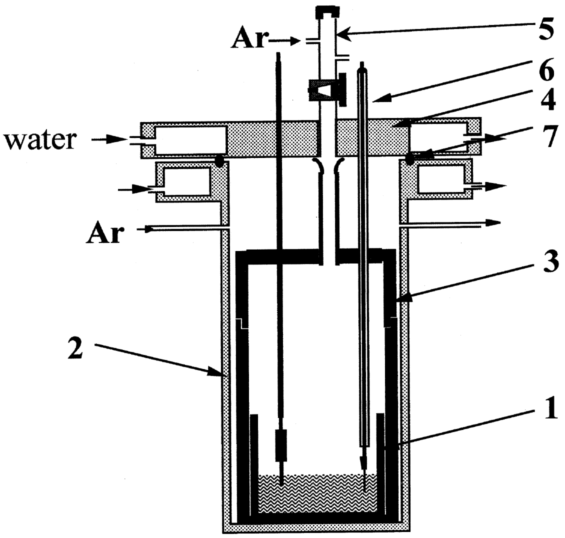

Fig. 1. Experimental cell: (1) vitreous carbon crucible; (2) refractory steel chamber; (3) graphite liner; (4) water-cooled lid; (5) inlet lock; (6) electrodes; (7) seal.

Various cathode materials were used: a 2 cm^2 stainless steel 304 sheet, steel SEA 1028, copper and vitreous carbon rod (2 cm^2). The vitreous carbon crucible in contact with the uranium granules was used as anode and the comparison electrode was a platinum wire (1 mm diam) [9]. The setup is shown in Fig. 1.

2.2. Characterization of the uranium deposit

After the electrolysis run, the cathode was covered with a mixture of dendritic uranium and salt attached to the dendrites, which was first weighed as a whole. Washing the cathode in an ultrasound tank containing a water ethanol solution dissolved the salt and detached the dendrites from the cathodic material. They were dried and weighed. The compactness of the uranium coating was measured by the ratio of the weight of uranium alone over the overall deposit weight. The weight of uranium was used to calculate the current efficiency of the electrolysis run. The dendrites were collected on an adhesive pellet and observed by scanning electron microscopy (LEO S440). A thin compact layer of uranium or uranium compound remained at the surface of the cathode. The cross-section of this layer was examined by energy dispersive spectroscopy (Oxford Link System) and by X-ray diffraction (Siemens D500).

2.3. Optimal design

In order to optimize the experimental conditions for the preparation of uranium deposit, rather than using the traditional approach, consisting in studying each factor separately, we used the 'optimal design methodology' where an optimal (in the statistical sense) matrix of experiments allows the factors to be varied simultaneously [11].

In this study, the aim was to assess the dependence of each of the three responses called y_i:

- the morphology of the deposit: smooth coatings, dendrites (qualitative response).
- the compactness of the deposit (quantitative response),
- the current efficiency of the electrolysis (quantitative response).

with respect to three factors: current density (CD), uranium ion content (UC), temperature (TEMP).

Since we chose a 'face centred central composite design' [12] (Table 1), the experimental domain is represented, in a three-dimensional coded space, by a cube (Fig. 2) where eight points are located at the corners (the factorial design points), six lie on the centre of the faces (star matrix points) and one at the centre of the cube (centre point). All the runs were duplicated except the centre point which was performed in triplicate. So, 31 runs had to be done; during the experiment, CD was varied between 50 and 400 mA cm^{-2} while UC from 3 to 5 mass% and TEMP 670–710°C. The experiments are reported in Table 1.

3. Experimental results and comments

For the optimal design experiments, the cathode was a steel sheet (SEA 1028), each electrolysis run was performed using 600°C, yielding a theoretical mass of 0.5 g pure deposited uranium.

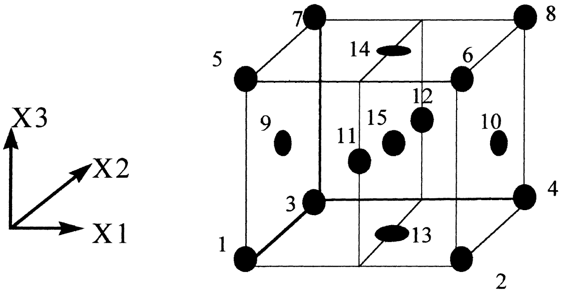

Fig. 2. Scheme of the optimal design model.

3.1. Influence of the electrokinetic parameters

3.1.1. The deposit morphology

After each of the 31 runs performed, the deposits were observed by SEM. Two types of dendrites, referred to as type 1 and type 2 were observed; they are shown in the micrographs in Figs. 3 and 4, respectively. Dendrite 1 presents a primary arm and secondary arms perpendicular to it. Dendrite 2 is also ramified but is more compact than type 1 and appears to be twinned. Fig. 5 shows the type of dendrite obtained in each experimental condition. The dendrite shape seems to depend on the temperature. Indeed, at 670°C, only type 1 was present, whereas at 710°, the dendrites were type 2. At the intermediate temperature, 690°C, either or both can be observed (hatched plane Fig. 5). To explain the existence of a transition temperature between two types of dendrite, the following assumption can be proposed: Uranium exists in two crystal structures α (orthorhombic) and β (tetragonal), only α stable at lower temperatures can be observed at room temperature [13]. The α to β transition temperature at 1 atm. is about 668°C [13],

Table 1
Experimental conditions: current density, CD; melt temperature, TEMP and uranium ion content, UC

No.	X_1	X_2	X_3	UC (% mass)	TEMP (°C)	CD (mA cm^{-2})
1	−1	−1	−1	2	670	50
2	+1	−1	−1	5	670	50
3	−1	+1	−1	2	710	50
4	+1	+1	−1	5	710	50
5	−1	−1	+1	2	670	400
6	+1	−1	+1	5	670	400
7	−1	+1	+1	2	710	400
8	+1	+1	+1	5	710	400
9	−1	0	0	2	690	225
10	+1	0	0	5	690	225
11	0	−1	0	3.5	670	225
12	0	+1	0	3.5	710	225
13	0	0	−1	3.5	690	50
14	0	0	+1	3.5	690	400
15	0	0	0	3.5	690	225

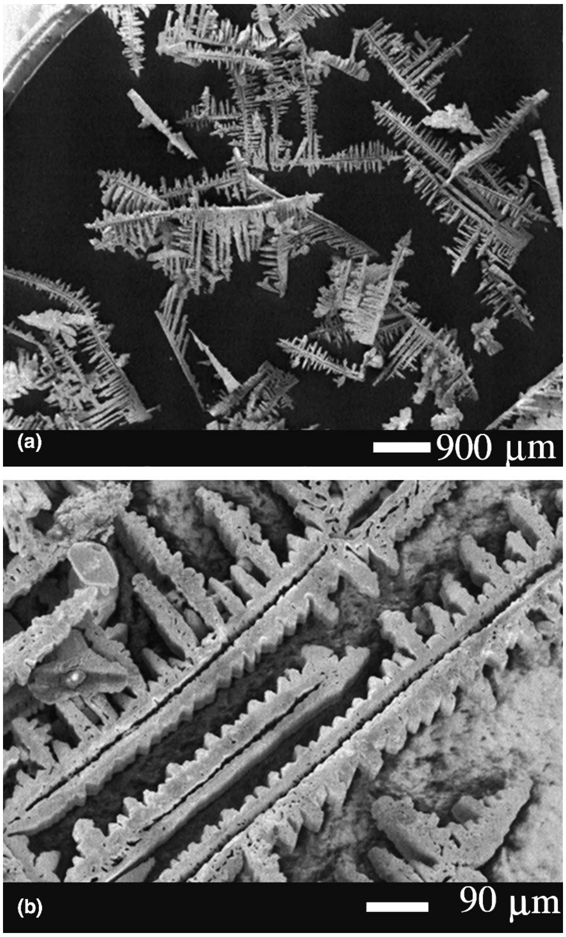

Fig. 3. SEM of type 1 uranium dendrites.

very close to our lower experimental temperatures. Dendrite type 1 provides from crystallization relevant to phase α and cooling of samples down to room temperature does not change the crystallographic structure of the deposit. Dendrite type 2 obviously grows following β structure and the cooling should promote sensibly the morphology of the deposit due to the transition β → α.

3.1.2. The current efficiency and the proportion of uranium in the coating

In Fig. 6(a) the current efficiency remains close to 100% and it is not influenced by the current density except at two points obtained at low current (83% and 78%). These experiments highlight that these working conditions may be suitable for industrial applications.

Fig. 6(b) displays the proportion of uranium in the coating obtained for each experimental point. It can be observed that the uranium mass was 30–35% of the total mass of the deposit, the rest was NaCl–KCl. Only for two points at 710°C the proportion was close to 50%.

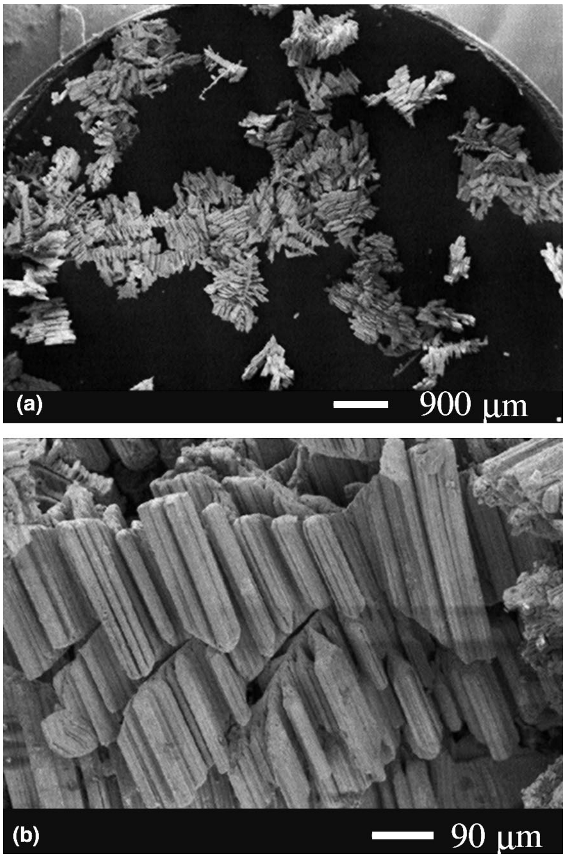

Fig. 4. SEM of type 2 uranium dendrites.

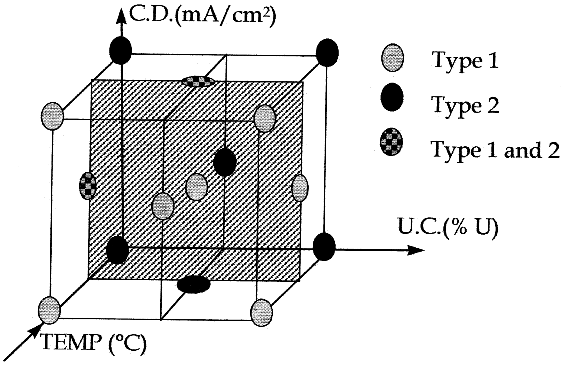

Fig. 5. Type of dendrite obtained for different conditions of the optimal design model.

This observation is coherent with those presented above: indeed, at the highest temperature, we observed that the dendrites were ramified and more compact, so that the insertion of salt was not as easy.

In each case, the results obtained had the same magnitude except two breaking points. Nevertheless, the

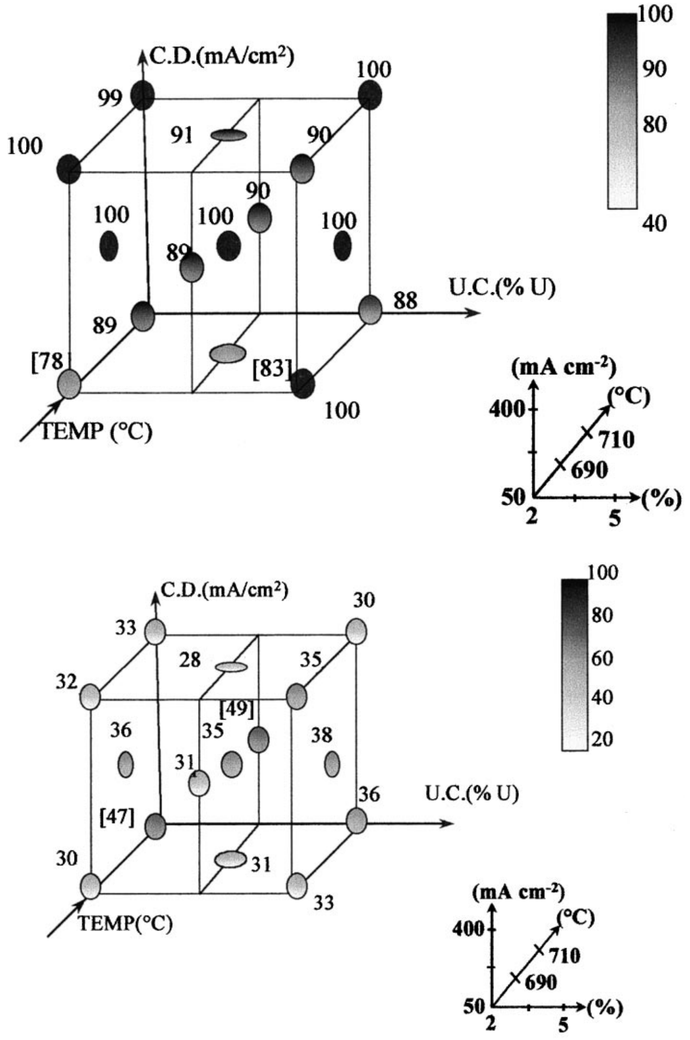

Fig. 6. Scheme of the results obtained: (a) current efficiency of the electrolysis, and (b) uranium rate in the deposit.

use of optimal design reveals important information on uranium deposition and gives results similar to those of the Argonne National Laboratory presented in Section 1 [3] which indicate that the parameters current density, temperature and concentration of the electrolyte have a moderate influence on the morphology of the uranium deposited. To explain this, we can assume that the compactness of the coating is mainly influenced by other phenomena not directly dependent on the electrolysis conditions such as: interactions between the deposited metal and the cathodic substrate or physical processes occurring during the growth of the metallic phase within the diffusion layer.

Additional experiments were performed in order to examine: (i) the influence of the substrate on the adherence of the deposit, (ii) the mode of growth of the coating during electrolysis.

3.2. Adherence of the deposit on various substrates

3.2.1. Experimental results

The cross-section of uranium coatings exhibits for various substrates an underlayer sensibly more compact and adherent than the upper part of the deposit; the adherence and the compactness of this underlayer depend strongly on the substrate, as observed by SEM (Figs. 7–10); the composition of this layer was determined by EDS and XRD:

(i) on steel (Fig. 7) there was a porous and quite adherent layer of pure uranium, of 4 μm thickness for a 600 C electrolysis; on vitreous carbon this layer was also pure uranium and of about 75 μm thickness for a 1200 C electrolysis (Fig. 8),

(ii) on copper (Fig. 9), there was a very compact and adherent layer of Cu_5U compound. In the case

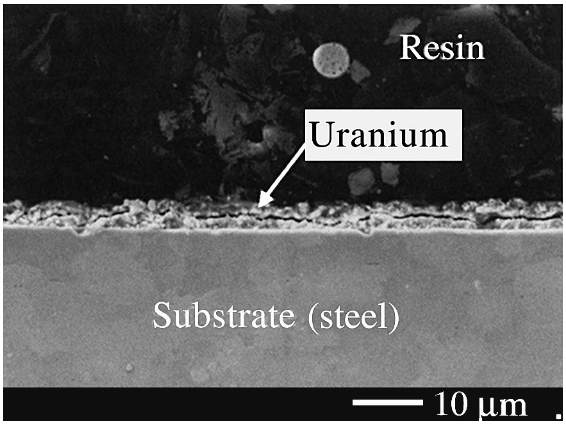

Fig. 7. SEM of electrode cross-section covered with resin, electrolysis conditions: UC = 5% mass, substrate steel SEA 1028, TEMP = 690°C, CD = 225 mA cm^{-2}, Q = 600 C.

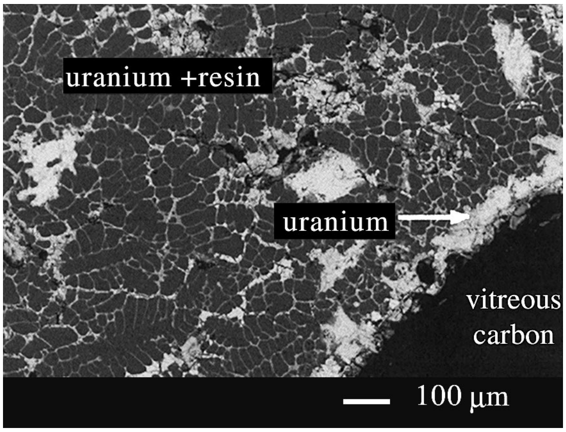

Fig. 8. SEM of electrode cross-section covered with resin, electrolysis conditions: UC = 3% mass, substrate steel SEA 1028, TEMP = 680°C, CD = 50 mA cm^{-2}, Q = 1200 C.

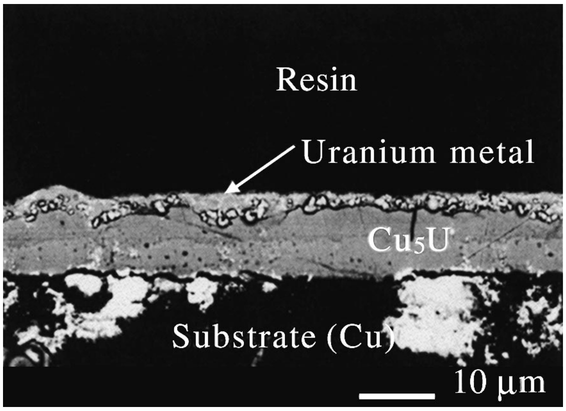

Fig. 9. SEM of electrode cross-section covered with resin, electrolysis conditions: UC = 5% mass, substrate steel SEA 1028, TEMP = 690°C, CD = 225 mA cm^{-2}, Q = 600 C.

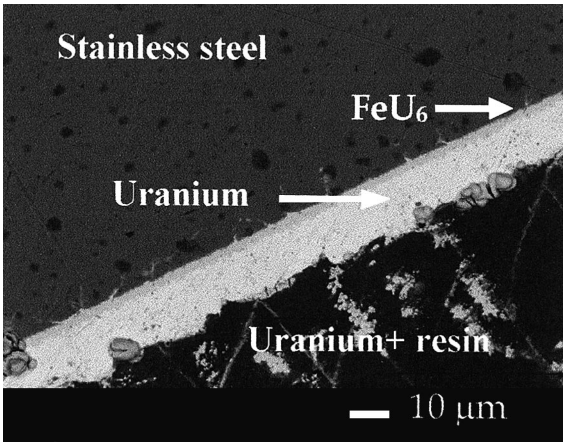

Fig. 10. SEM of electrode cross-section covered with resin, electrolysis conditions: UC = 5% mass, substrate steel SEA 1028, TEMP = 680°C, CD = 33 mA cm^{-2}, Q = 600 C.

of stainless steel it was divided in two strata: a thin layer of U_6Fe (2 µm) at the substrate interface and above a compact layer of pure uranium (Fig. 10).

3.2.2. Discussion

Uranium deposition on various substrates can be divided into two steps:

(i) a thin layer is deposited on the substrate,

(ii) dendrites attach to this thin layer.

Adherence depends directly on the reactivity between the uranium and cathode material. There is strong reactivity when intermetallic compounds like UCu_5 or U_6Fe are formed by interdiffusion. Moreover, note that Marshall [4] observed a UNi_5 interface with a nickel cathode in NaCl–KCl–UCl_3 at 800°C. The presence of an underlayer is correlated with good adherence of the dendrites. Conversely, on a steel and on vitreous carbon, there is a low reactivity between uranium and the substrate. In the case of vitreous carbon, the formation of uranium carbide is thermodynamically forbidden. In the case of steel, the low reactivity with iron is due to the low temperature. The presence of Ni in stainless steel makes it possible to lower the temperature of the reaction and diffusion.

3.3. Dendrite growth during electrolysis

Previous studies on electrochemical nucleation of uranium [10] have shown that, in the early stages of electrolysis, the initial nuclei are created instantaneously. Thus, the first nuclei grow simultaneously so grains of uniform size are observed after electrolysis times of less than 1 s.

The micrographs presented in Figs. 11–13, show the surface of the cathode after electrolysis of, respectively,

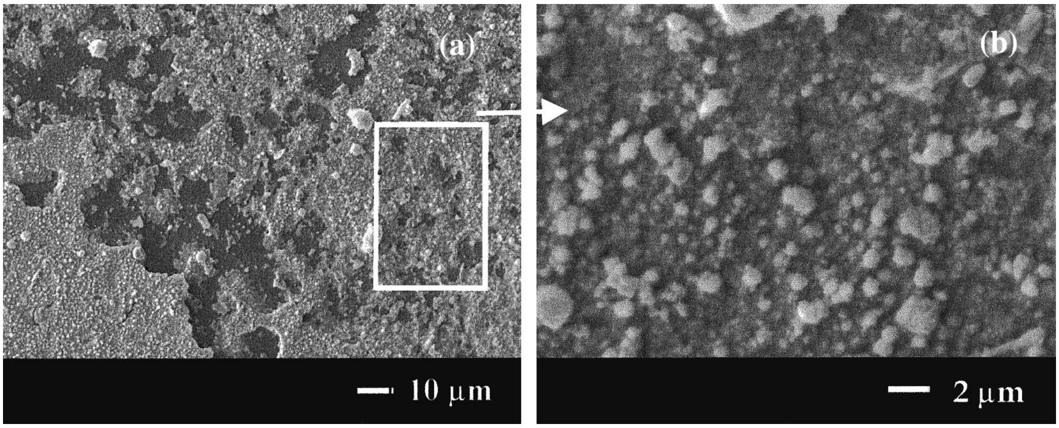

Fig. 11. SEM of uranium deposit obtained by a short electrolysis: 44 s (charge: 20C) Electrolysis conditions: substrate steel, TEMP = 690°C, CD = 225 mA cm^{-2}.

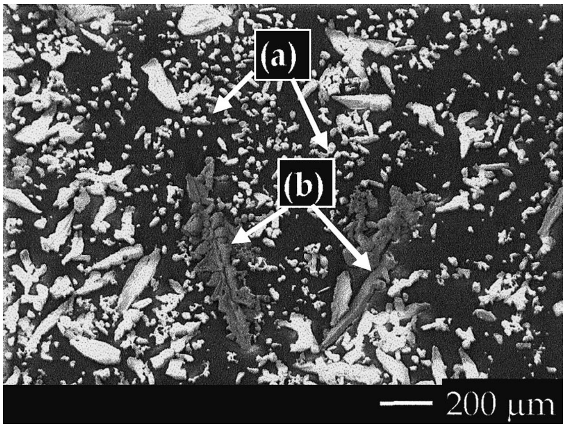

Fig. 12. SEM of uranium dendrites (cleaned and dried), electrolysis conditions: substrate steel, TEMP = 690°C, CD = 225 mA cm^{-2}, $Q = 80$ C.

45 s, 3 and 7 min corresponding to charges of 20, 80 and 200 C.

(i) charge = 20 C (Fig. 11): A thin layer of uranium is observed on the cathode (Fig. 11(a)), we note that some parts of the substrate are not covered (dark zones). Magnification of this layer shows that it is composed of nodules (Fig. 11(b)).

(ii) charge = 80 C: The micrographs in Fig. 12 show that the surface of a uranium deposit obtained after 3 min of electrolysis is no longer homogeneous, including two kinds of crystals:

- small grains of quite uniform size (Fig. 12(a)) which seem to result from the initial germination process;
- dendrites with varying degrees of ramification, present (Fig. 12(b)) clearly resulting from an additional physical process. This second process finally predominates.

(iii) charge = 200 C: Here the substrate is entirely covered with a layer of uranium and some faceted

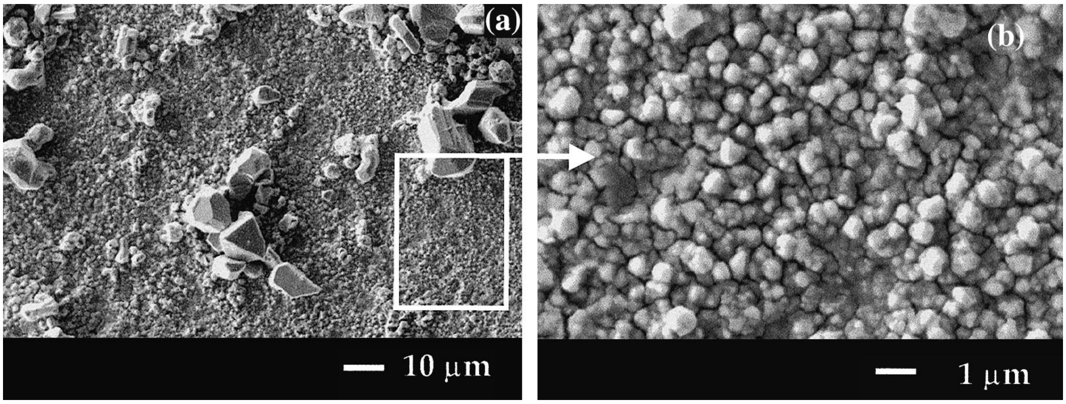

Fig. 13. SEM of uranium deposit obtained by electrolysis: 7 min (charge: 200C). Electrolysis conditions: substrate steel, TEMP = 690°C, CD = 225 mA cm^{-2}.

prominences appear which could be the base of dendrites (cf. Fig. 13(a)). Similar prominences had been observed in analogous conditions by Chauvin et al. [14].

At the magnification of Fig. 13(b) we see that it is composed of an agglomerate of grains of homogeneous size. These grains arise from the growth of the nodules observed in the micrograph in Fig. 11. The comparison of these two micrographs reveals that the increase in size of these nodules is anomalously low. However, this can be explained by the fact that most of the current is used for the growth of the dendrites.

3.4. Discussion on dendrite phenomena

Dendrite formation is generally attributed to the diffusion of depleted electrolyte on the electrode surface which promotes a tertiary current distribution. Other physical phenomena occurring during electrodeposition should also be taken into account to explain the particularities of uranium electrodeposition i.e. the instantaneous dendrite growth in any electrokinetic conditions, their ramified morphology, the irregularity of the deposit thickness.

For this discussion, we will refer to recent papers which report on phenomena concerning the development of dendritic coatings in aqueous media.

Firstly, let us consider the beginning of the growth of the layer, just after nucleation: Budevski et al., have proposed models taking into account the binding energy of the electrodeposited metal (M), either on substrate (S), Ψ_{MS} or on the predeposited metal $\Psi_{\mathrm{M-M}}$ [15,16]. When $\Psi_{\mathrm{M-S}} \ll \Psi_{\mathrm{M-M}}$ (Volmer–Weber model), M becomes deposited on M rather than on S, leading to three-dimensional islands. This initial process favors the rapid formation of axial dendrites on the cathode surface. Obviously it corresponds to uranium electrocoating on steel.

With copper, a surface alloy is formed by metal interdiffusion with the underlayers of uranium and dendrite formation occurs when the intermetallic layer is saturated; at this time $\Psi_{\mathrm{M-M}}$ is higher than $\Psi_{\mathrm{M-alloy}}$ and once again, M forms 3D islands. This situation is predicted by the model of Stranski–Krastanov [15,16].

During coating growth, orthogonal needles result from diffusional phenomena favouring current at the top of the islands. At this stage, the heterogeneity of the electrolyte layer at the interface with the cathode material causes a particular fluid motion which readily influences the morphology of the coating. Recent articles deal with these particularities, observed in aqueous electrodeposition [17–21].

Fleury et al. [17] demonstrated that the depletion of cations near the cathode generates strong local electric fields. According to these authors, the electrolyte motion follows contrarotative vortices at the tip of each needle, producing ramification at the edges. Obviously this phenomenon, repeated at each tip, leads to a coating with an arborescent morphology and fractal properties. Experimental visualization of contrarotative vortices and the dendrite growth modes were reported by Huth et al. [20].

Another phenomenon can explain that on a vertical cathode, the coating is thicker at the bottom than at the top and that dendrite growth is rather thicker in the bottom of the crucible: the discharge of uranium ions at the cathode promotes a significant change in the density of the electrolyte because of the high atomic mass uranium. The depleted solution is lighter than the bulk solution and rises to the surface whereas at the anode, the oxidation process produces a heavier solution falling in the electrolyte. So, mass transfer and therefore deposit growth is favoured in the lower part of the cathode where the more concentrated solution is.

These theoretical considerations seem to agree with our observations on uranium electrodeposition (although any visual verification is impossible in this case) and so can be accepted for the interpretation of our results.

We observed that dendrites cannot be avoided by changing the electrokinetic parameters. A possible solution could be the use of pulsed currents: during the on-time the convective processes are only in their beginning period and during the off-time the heterogeneities created in the diffusion layer would disappear, so that a net improvement can be expected in the overall process. Marshall et al. [4] obtained more compact uranium coatings using this method.

4. Conclusion

Our work, initially focused on the conditions of preparing compact coatings of uranium, has shown that the deposits of this metal by electrodeposition in molten chlorides are dendritic. Several experimental runs, carried out in an optimal design, demonstrated that only the temperature has a moderate effect on the compactness of the coatings, whereas other parameters such as the current density and the uranium ion content, which are critical in other electrodeposition systems, do not influence the crystallographic properties of the uranium coatings. Similar features were observed by other authors preparing uranium coatings at lower temperatures.

Nevertheless, this work reveals two original aspects: (i) the cathodic substrate influences the adherence of the coating, due to specific interface properties leading in certain cases (copper, stainless steel) to alloy sublayers; (ii) dendrites are metallic protrusions, formed at the early stages of the electrodeposition runs, growing much faster than the other crystals.

Dendrite formation is favoured by the diffusion of the electrolyte occurring as soon as the protrusions appear; besides, a fractal structure is evidenced and attributed to other transfer phenomena, namely electroconvection and migration at the cathode interface which are specific both to the shape of the growing dendrites and the electrolyte properties.

Identical phenomena were identified and characterized in aqueous electrodeposition systems. We intend to follow this work by similar detailed investigations in molten salt, taking into account the specific properties of uranium electrodeposition baths, enabling the process to be modelled.

Acknowledgements

The authors express their thanks to the Cogema Compagny and in particular to G. Sauzay for their collaboration and support in this research.

References

[1] F.H. Driggs, W.C. Lilliendahl, Ind. Eng. Chem. 22 (5) (1930) 516.

[2] M. Kolodney, US Patent 2,777,809 (1957).

[3] C. Marzano, R.A. Noland, Report ANL-5102, Argonne National Laboratory, 1953.

[4] S.L. Marshall, L. Redey, G.F. Vandegrift, D.R. Vissers, Report ANL-89/26, Argonne National Laboratory, 1989.

[5] T.C. Totemeier, R.D. Mariani, J. Nucl. Mater. 250 (1997) 131.

[6] L. Lopez-Tomas, J. March, P.P. Trigueros, F. Mas, J. Claret, F. Sagues, Chaos, Solitons & Fractals 6 (1995) 287.

[7] J.L. Barton, J.O'M. Bockris, Proc. Roy. Soc. A 268 (1962) 485.

[8] J.W. Diggle, A.R. Despic, J.O'M. Bockris, J. Electrochem. Soc. 116 (11) (1969) 1503.

[9] K. Serrano, P. Taxil, J. Appl. Electrochem. 29 (4) (1999) 497.

[10] K. Serrano, P. Taxil, J. Appl. Electrochem. 29 (4) (1999) 505.

[11] G.E.P. Box, W.G. Hunter, J.S. Hunter, Statistic for Experimenters: An Introduction to Designs, Data Analysis and Model Building, Wiley, New York, 1978.

[12] G.E.P. Box, N.R. Drapper, Empirical Model-Building and Response Surfaces, Wiley, New York, 1987.

[13] J.J. Katz, E. Rabinowitch, The Chemistry of Uranium The Element, Its binary and Related Compounds, Dover, New York, 1951.

[14] G. Chauvin, H. Coriou, P. Jabot, A. Laroche, J. Nucl. Mater. 11 (2) (1964) 183.

[15] W.J. Lorenz, G. Staikov, Surf. Sci. 335 (1995) 32.

[16] E. Budevski, G. Staikov, W.J. Lorenz, Electrochemical Phase Formation and Growth, VCH Publications, New York, 1996.

[17] V. Fleury, J.N. Chazalviel, M. Rosso, Phys. Rev. E 48 (2) (1993) 1279.

[18] V. Fleury, J.H. Kaufman, D.B. Hibbert, Nature 367 (3) (1994) 435.

[19] D.P. Barkey, D. Watt, Z. Liu, S. Raber, J. Electrochem. Soc. 141 (5) (1994) 1206.

[20] J.M. Huth, H.L. Swinney, W.D. McCormick, Phys. Rev. E 51 (4) (1995) 3444.

[21] F. Argoul, E. Freysz, A. Kuhn, C. Léger, L. Potin, Phys. Rev. E 53 (2) (1996) 1777.